

Two-photon processes in faint biphoton fields

Dmitry V. Strekalov, Matthew C. Stowe, Maria V. Chekhova*
and Jonathan P. Dowling.

Quantum Computing Technologies Group, Sect. 367,
Jet Propulsion Laboratory, California Institute of Technology,
MS 300-123, 4800 Oak Grove Drive, Pasadena, CA 91109.

Dmitry.V.Strekalov@jpl.nasa.gov

*Moscow State University,
Moscow, Russia

October 23, 2018

Abstract

The goal of this research is to determine and study a physical system that will enable a fast and intrinsically two-photon detector, which would be of interest for quantum information and metrology applications. We consider two types of two-photon processes that can be observed using a very faint, but quantum-correlated *biphoton* field. These are optical up-conversion and an external photoelectric effect. We estimate the correlation enhancement factor for the biphoton light compared to coherent light, report and discuss the preliminary experimental results.

1 Introduction

The term “biphoton” has been suggested by D.N. Klyshko [1] for describing systems of entangled photon pairs, such as those produced in the Spontaneous Parametric Down Conversion (SPDC) of light¹. In this process, a pump photon is coherently converted into a pair of entangled photons in a $\chi^{(2)}$ medium [2], while the phase and spectral properties of the pump are transferred to the biphoton [3, 4]. This phase then can be recovered by a two-photon correlation measurement. In this context, describing this system as “two photons” is not complete and even may be misleading as it tends to omit the quantum correlation properties of the photon pair [5, 6]; so the term “biphoton” proves to be very useful.

A pair of entangled particles that are space-like separated is an excellent system for testing the concepts of physical *locality* and *reality* [7]. Therefore it is not surprising that SPDC has received great attention as an entanglement source for Bell inequalities tests. The whole variety of such tests can be generally described as nonlocal biphoton interference experiments. As a further development, experiments involving higher-order interference have been carried out, such as the Greenberger-Horne-Zeilinger theorem test [8] and quantum teleportation [9, 10].

Besides purely a fundamental interest, study of the biphoton light has inspired development of new information and measurement technologies, such as quantum cryptography [11], sub-shot noise optical phase measurements [12–14], quantum clock synchronization [15, 16], and others. Most recently, the possibility of sub-diffraction-limited imaging [14] and lithography [17–21] has been discussed. There is a clear shift of the research in biphoton optics towards practical applications. It is also clear that the difficulties on the path to such applications are quite severe and have one common root, which is the detection problem.

Consider quantum cryptography, which is generally believed to be the most mature of quantum optical technologies. It has been shown [22] that the main limitation blocking its practical implementation is the single-photon detection rate. It is not possible, with the state-of-art single-photon detectors, to achieve the detection rate that would make useful wideband quantum crypto-communication channels [22]. Similarly, quantum optical interferometers are theoretically capable of being noise-limited at the fundamental (Heisenberg) level $1/\langle n \rangle$, while the classical shot-noise limit is $1/\sqrt{\langle n \rangle}$ ($\langle n \rangle$ being the mean number of photons per measurement). Therefore the quantum measurement of the phase has advantage over the classical one only when $\langle n \rangle$ is large. But for a large photon flux, any coincidence detection technique will fail because of the finite dead time of photon counting detectors and coincidence circuit time-windows. Thus again, the detection rate of photon pairs is the limiting factor. The situation gets even more complicated for quantum lithography, where the two-photon detectors are molecules in the resists that are small and distributed in the media. Here one has to worry not only about the detection rate, or fast

¹In acknowledgment of D. N. Klyshko’s founding role in studies of parametric processes in optics, SPDC is sometimes referred to as “Klyshko radiation”.

two-photon sensitivity, but also about the transverse correlation properties of the biphoton light.

Therefore the search for fast two-photon processes that could enable a true two-photon detector (as opposed to an electronic coincidence circuit), that could be used for study of strong biphoton fields, becomes one of the most important questions of the applied quantum optics. So far, no two-photon processes induced by the biphoton field have been demonstrated, although a much brighter radiation consisting of photon pairs from optical parametric oscillator (OPO) has been shown to be more efficient for second harmonic generation [23] and for two-photon ionization of atoms [24,25] than the ordinary coherent radiation. On the other hand, two-photon processes in strong classical fields, such as pulsed laser fields, have been studied quite extensively.

The goal of our research is to analyze the possibility of direct two-photon detection of the biphoton field and to determine the physical system which is most suitable for this purpose. In the following sections we will demonstrate the advantage of biphoton light over coherent light for driving two-photon processes. This advantage will be shown considerable enough to make up for extremely low power of the biphoton sources such as SPDC. Then, we will discuss two types of processes that could serve for direct two-photon detection: optical up-conversion and the photo-electric effect.

2 Photon detection in biphoton and coherent fields

We will use a conventional concept of a photon detection event [26], which takes place with a probability proportional to a constant η (the *quantum efficiency* of the detector) and to the probability to have at least one photon in the detection volume V . This volume can be generally defined in phase space as $V = \Delta k_x \Delta k_y \Delta k_z \Delta x \Delta y \Delta z$, just like the phase-space volume occupied by radiation from a source. For example, in the (x, p_x) subspace of the phase space, a point-like detector may be represented as a vertical line, whereas a distributed but wavelength selective detector (a bandpass filter) will be represented as a horizontal line. If the source or the detector are single-mode, then their x- and k-volumes are reciprocal to each other, and $V = (2\pi)^3$. Therefore the number of modes a detector can see, or a source can radiate, can be calculated as

$$M = \frac{V}{(2\pi)^3} = \frac{AL}{(2\pi)^3} \frac{k^2}{c} \Delta\Omega \Delta\omega, \quad (1)$$

where for the x-part of V we substitute a product of the detector's cross section A and its length L , and for the k-part we take

$$\Delta k_x \Delta k_y \Delta k_z = k^2 \Delta\Omega \Delta k = \frac{k^2}{c} \Delta\Omega \Delta\omega. \quad (2)$$

In Eqs. (1) and (2), $\Delta\Omega$ and $\Delta\omega$ are the solid angle and frequency ranges, respectively, and c is the speed of light.

Knowing the definition of the “detection event” and associated with it phase-space volume, we can estimate detection rate for radiation with known properties. For example, in the next section we will consider optical up-conversion process, which is the reverse of the SPDC process, as a two-photon detector. A peculiarity of such a detector is that the phase space volumes for two up-converting photons are different. Any *signal* photon can be up-converted anywhere within the illuminated part of the crystal (the x-volume) and within the k-volume whose (λ, θ) section is shown as a tuning curve in Fig.1. But the up-conversion only may take place in presence of the *idler* photon satisfying the phase matching conditions with the signal photon:

$$\begin{aligned}\omega_s + \omega_i &= \omega_p, \\ \vec{k}_s + \vec{k}_i &= \vec{k}_p,\end{aligned}\tag{3}$$

where ω_p and \vec{k}_p are the frequency and wave vector of the pump. The choice which photon is the signal and which one is the idler is arbitrary, just like in SPDC.

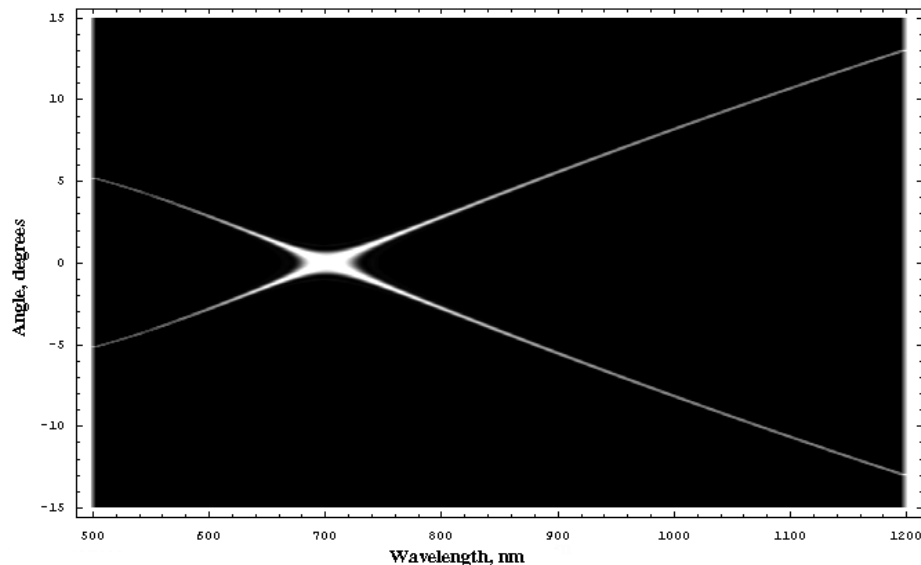


Figure 1: The SPDC spectrum for a 5 mm Type-I BBO cut for the collinear degenerate phase matching.

The phase space volume for a signal photon contains a large number M of modes, however the phase space volume for the *phase-matching* idler photon is transform-limited in all directions for a single-mode pump. Hence this volume is equal to $(2\pi)^3$ and contains only one mode. In the limit of weak fields, $\langle n \rangle \ll 1$, both volumes are filled with at least one photon each with probability $M \langle n \rangle \times \langle n \rangle$. When this condition is fulfilled, a detection occurs with probability $\eta^{(2)}$ which absorbs the quantum efficiencies of non-linear up-conversion and of subsequent photo detection. Therefore the two-photon detection probability from a coherently illuminated up-conversion detector can be estimated as

$$R_{coh} = \eta^{(2)} M \langle n \rangle^2 .\tag{4}$$

Even though the detector we describe is capable of seeing a large number M_{spdc} of modes, not all of them may be filled by the radiation source. In practice, the laser sources used in the up-conversion and second harmonic generation experiments are well collimated and have a relatively narrow frequency band width. Therefore in Eq. (4), we should take the number of modes of a laser source $M = M_{laser}$.

Now instead of coherent light let us consider the biphoton light. The most important distinction is that under proper imaging conditions (more detail in the next section), for every signal photon the phase-matched idler photon is guaranteed to be present, so the detection volumes are filled with at least one photon each with probability $M \langle n \rangle$. In contrast with Eq. (4), in this case $M = M_{spdc}$, and instead of (4) we get

$$R_{spdc} = \eta^{(2)} M_{spdc} \langle n \rangle. \quad (5)$$

Comparing the two-photon signal from coherent light (4) and from biphoton light (5) we can determine how much biphoton light is more efficient than coherent light for the type of two-photon process we presently consider. This comparison can be carried out either for equal intensities, or for equal $\langle n \rangle$. We will carry it out for equal intensities, since this will allow for a direct comparison with known experiments.

The mean number of photons per mode $\langle n \rangle$ can be expressed in terms of brightness as [27]

$$\langle n \rangle = \frac{I\lambda^3}{\hbar c} \frac{1}{\Delta\Omega\Delta\omega}, \quad (6)$$

where I is intensity. Multiplying (6) by (1) we get the following equation:

$$M \langle n \rangle = \frac{IAL}{c\hbar\omega}, \quad (7)$$

which appears rather obvious, since its left side is the mean total number of photons, and the right side is the total energy of radiation divided by the energy of a photon.

Now we can directly compare the signals from coherent and biphoton fields:

$$\xi \equiv \frac{R_{spdc}}{R_{coh}} = \frac{M_{spdc} \langle n \rangle_{spdc}}{M_{coh} \langle n \rangle_{coh}^2}. \quad (8)$$

Substituting (6) and (7) in (8) and assuming $I_{spdc} = I_{coh} \equiv I$, we find

$$\xi = \frac{\hbar c \Delta\Omega_{coh} \Delta\omega_{coh}}{I\lambda^3}. \quad (9)$$

Now let us make numeric estimates. We consider a Type-I BBO crystal near collinear degenerate phase matching with the central wavelength $\lambda_0 = 702$ nm, whose spectrum is shown in Fig.1. The typical light power we get from a 5 mm - long Type-I BBO crystal is 50 nW. This SPDC light is generated by the pump beam that is approximately 100 microns in diameter. This gives us $I \approx 5$ W/m². For comparison, we will take a mode-locked pulsed laser with pulse width of 150 fs ($\Delta\omega_{coh} \approx 4 \times 10^{13}$ s⁻¹) and duty cycle of 10⁻⁵. This laser is

focused into a $100 \mu\text{m}$ spot with near-diffraction divergence of $\theta_d \approx \lambda/d \approx 5 \times 10^{-5}$ radians, which gives us $\Delta\Omega \approx 2\pi\theta_d^2 \approx 3 \times 10^{-4}$ st. radians. Substituting these numbers into Eq. (9) we obtain $\xi \approx 200$. It is easy to see that an estimate carried out for $\langle n \rangle_{spdc} = \langle n \rangle_{coh}$ (and valid when both types of radiation have similar spectral width and divergence) gives a much larger value of ξ .

3 Up-conversion of biphoton field

Up-conversion of strong coherent fields is routinely used in optical autocorrelators to measure the duration of short pulses. The large value of the enhancement factor ξ for the biphoton light suggests that the optical up-conversion can be observed with such light, despite a typically very low efficiency of this process. It should be possible, using a pair of similar nonlinear crystals (the first one for SPDC and the second one for the up-conversion), to detect the up-converted UV photons emitted from the second crystal. Fig.2 is a conceptual drawing of a system which brings back together all photon pairs emitted from a localized source at various angles, while preserving the phase-matching conditions (that are equivalent for SPDC and for the up-conversion) by an imaging system with a unity magnification. This system is represented by a lens placed between the two nonlinear crystals at the distance $2f$ from each.

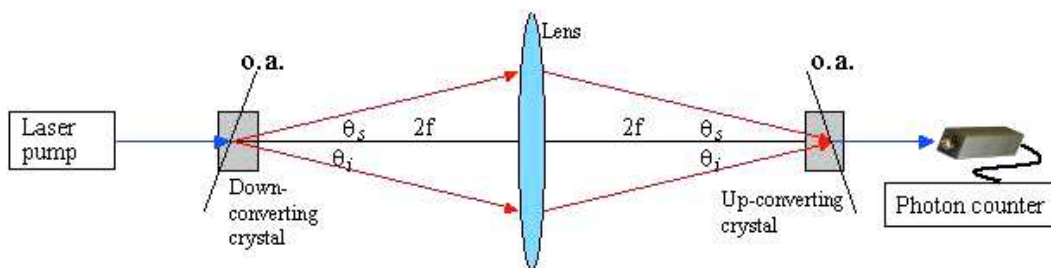


Figure 2: A conceptual drawing of the experiment on up-conversion of biphoton light. O.A. stands for the optical axes of the nonlinear crystals.

A rough estimate of the expected detection rate of the up-converted UV photons can be carried out based on the above-found biphoton enhancement factor and on the experimental observation that a 1 Watt laser pump such as described in the previous section focused down to about 100 microns on a BBO crystal similar to the one we use for up-conversion produces approximately 600 mW of the second harmonic. Scaling this number quadratically to a 50 nW pump power and multiplying by the duty cycle to obtain an estimate for CW, we get 1.5×10^{-20} W of the up-converted light, or about 0.2 photons per second. To take the biphoton nature of our “pump” into account, we multiply this number by the enhancement factor ξ , arriving at 40 photons per second. Such a signal should be detectable with a low-noise photomultiplier tube with a few percent quantum efficiency. However, this number gets significantly lower if a more careful evaluation is carried out, and various mechanisms

of the phase mismatch are taken into account. To perform such an evaluation we need to understand the transverse correlation properties of a biphoton.

While the longitudinal (temporal) correlation in the biphoton field has been extensively studied in both theory and experiment, starting from the pioneering works [28, 29], the studies of its transverse correlation are few. A very broad theoretical description is given in [30]; theoretical analysis along with experimental data is also presented in [3]; study of biphoton propagation through generic imaging systems is reported in [31, 32].

Summarizing the analysis from [3], we write the quantum state of a biphoton emitted in a monochromatically pumped SPDC process as

$$|\Psi\rangle = \int F(\vec{k}_s, \vec{k}_i) |1\rangle_{\vec{k}_s} |1\rangle_{\vec{k}_i} d\vec{k}_s d\vec{k}_i, \quad (10)$$

where the delta-like two-photon amplitude $F(\vec{k}_s, \vec{k}_i)$ which entangles the signal SPDC mode labelled by its wave vector \vec{k}_s with the idler mode \vec{k}_i breaks up into a product of its longitudinal and transverse parts:

$$F(\vec{k}_s, \vec{k}_i) = F_x(\Delta\omega, \Delta\theta_s, \Delta\theta_i) F_z(\Delta\omega, \Delta\theta_s, \Delta\theta_i). \quad (11)$$

In Eq. (11), the arguments of the two-photon amplitude F , representing the wave vectors and frequencies of the signal and idler photons, are first replaced by the variations of these values from their central values that satisfy the phase matching conditions (3) so that

$$\begin{aligned} \Delta\omega &\equiv \omega_s(\vec{k}_s) - \omega_{s0}(\vec{k}_{s0}) = \omega_{i0}(\vec{k}_{i0}) - \omega_i(\vec{k}_i), \\ \Delta\vec{k}_s &\equiv \vec{k}_s - \vec{k}_{s0}, \\ \Delta\vec{k}_i &\equiv \vec{k}_i - \vec{k}_{i0}. \end{aligned} \quad (12)$$

Then, the longitudinal (z) and transverse (x) components of the phase mismatch $\Delta\vec{k}_s + \Delta\vec{k}_i$ are expressed via $\Delta\omega$ and the variations of the angles $\Delta\theta_{s,i}$ to result into the expressions for the F_x and F_z in Eq. (11).

The physical meaning and the use of the two-photon amplitude (11) is quite transparent. One can set $\Delta\theta_{s,i} = 0$ and study only the temporal, or longitudinal, correlation of the biphoton. This is often done since such an approximation describes the most usual type of experiments with SPDC, when the signal and idler modes are selected by a set of narrow pinholes. On the other hand, one could collect the biphoton light from a broad range of angles, but through a pair of very narrow band-pass optical filters. This case corresponds to the limit $\Delta\omega = 0$ which gives the angular, or transverse, part of the biphoton amplitude, which we need to find.

As it has been shown in [3], F_x reflects the properties of the pump angular spectrum and the transverse inhomogeneities of the crystal; it has a Gaussian shape for a Gaussian shaped pump. F_z depends on the polarization and wavelength dispersion properties of the nonlinear crystal. The analysis for a monochromatic Gaussian pump of the diameter a and for a Type-I crystal of the length l yields simple expressions for F_x and F_z as functions of

the internal angles $\theta^{(in)}$. Assuming $\Delta\omega = 0$ we have

$$\begin{aligned}
 F_x &= \exp \left\{ -\frac{(2\pi a)^2}{4} \left(\frac{n(\lambda_s)}{\lambda_s} \cos[\theta^{(in)}(\lambda_s)] \Delta\theta_s^{(in)} - \frac{n(\lambda_i)}{\lambda_i} \cos[\theta^{(in)}(\lambda_i)] \Delta\theta_i^{(in)} \right)^2 \right\}, \\
 F_z &= \text{sinc} \left\{ -\frac{2\pi l}{2} \left(\frac{n(\lambda_s)}{\lambda_s} \sin[\theta^{(in)}(\lambda_s)] \Delta\theta_s^{(in)} + \frac{n(\lambda_i)}{\lambda_i} \sin[\theta^{(in)}(\lambda_i)] \Delta\theta_i^{(in)} \right) \right\}. \quad (13)
 \end{aligned}$$

The wavelengths $\lambda_{s,i}$ correspond to k_{s0} and k_{i0} , and are related by the phase matching conditions (3) to each other and to the angles θ .

It is of interest to point out that F_x is a function of the angular variation differences, while F_z is a function of their sum. Therefore (considering the opposite signs of θ_s and θ_i) F_x defines the range of angles over which both the signal and idler differ from the exact phase-matching directions, while preserving the angle between them. The function F_z defines the range of variation of the angle between the signal and idler. This is similar to factorization of the temporal (longitudinal) part of the biphoton amplitude, which has been shown to break up as a product of functions of the sum and difference of two detection times: $u(t_1 - t_2) \times v(t_1 + t_2)$ [33]. In this case, v takes on the shape of the pump frequency spectrum (and is similar to F_x in the present study) and u depends essentially on the polarization and wavelength dispersion properties of the crystal (and is similar to F_z in the present study).

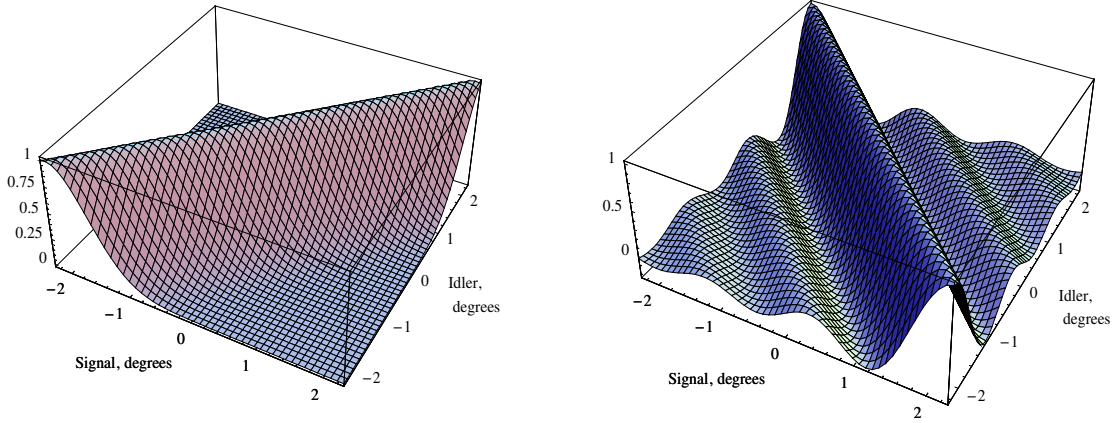


Figure 3: The transverse part of the biphoton amplitude $F_x(0, \Delta\theta_s, \Delta\theta_i)$ (on the left) and $F_z(0, \Delta\theta_s, \Delta\theta_i)$ (on the right). The signal and idler wavelengths are $\lambda_s = 690$ nm, $\lambda_i = 715$ nm.

The internal angles in Eq. (13) may be replaced by the external ones via the Snell's law. The results are shown in Fig.3 for the pair $\lambda_s = 690$ nm, $\lambda_i = 715$ nm. The product of $F_x(0, \Delta\theta_s, \Delta\theta_i)$ and $F_z(0, \Delta\theta_s, \Delta\theta_i)$ gives $F(0, \Delta\theta_s, \Delta\theta_i)$, whose absolute square can be interpreted as a correlation function of the angular variations $\Delta\theta_s$ and $\Delta\theta_i$. It turns out that the width of F_z strongly depends on the signal and idler wavelength variation from degeneracy (when $\lambda_s = \lambda_i$), getting broader as these wavelengths approach the degenerate

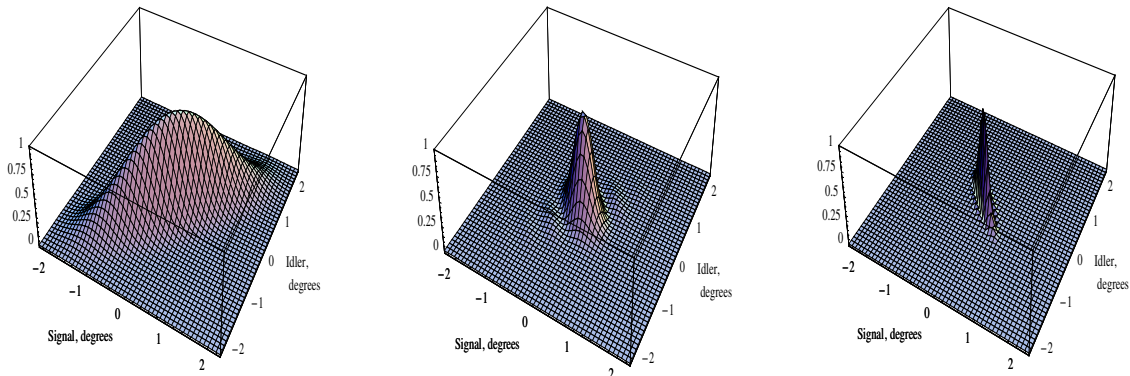


Figure 4: The biphoton transverse correlation functions $F^2(0, \Delta\theta_s, \Delta\theta_i)$. The signal and idler wavelengths are close to degeneracy (on the left); $\lambda_s = 690$ nm, $\lambda_i = 715$ nm (in the center); and $\lambda_s = 650$ nm, $\lambda_i = 754$ nm (on the right).

values. Three examples of $F^2(0, \Delta\theta_s, \Delta\theta_i)$ for different signal and idler wavelengths are shown in Fig.4, where the middle plot corresponds to the product of functions from Fig.3.

Understanding of the transverse correlation properties of biphotons allows for a more thorough analysis of the biphoton up-conversion experiment. In particular, it allows us to establish the required degree of precision in alignment of the crystals' optical axes. To do this we substitute the arguments of the correlation function $F^2(0, \Delta\theta_s, \Delta\theta_i)$ with the phase-matching angles variations:

$$\Delta\theta_{s,i} = \frac{\partial\theta_{s,i}}{\partial\alpha} \Delta\alpha, \quad (14)$$

where the derivative is calculated with respect to the angle α between the optical axis and the pump beam. The function obtained from substituting Eq. (14) into $F^2(0, \Delta\theta_s, \Delta\theta_i)$ represents the degree of overlap between the the down- and up-conversion phase matching conditions for crystals whose optical axes are misaligned by $\Delta\alpha$. In the following, we will call it the overlap function. Curiously, this function is practically uniform throughout the entire SPDC spectrum. Fig.5 shows two plots of this function: for degenerate, and for far non-degenerate wavelengths, that looks like a single line.

From Fig.5 we see that the crystals' optical axes need to be aligned to about 0.2° which is not hard to achieve. A bigger difficulty arises from the finite length of the crystals. Even though the parts of the down-converting crystal displaced from the 1:1 imaging plane still do get imaged onto the up-converting crystal, the signal and idler rays now cross at angles different from their phase matching angles θ_s, θ_i . These angular errors can be found from simple geometrical considerations as functions of the linear displacement z from the 1:1 imaging plane. Substituting them into $F^2(0, \Delta\theta_s, \Delta\theta_i)$ we find the overlap function as a function of z for different parts of the SPDC spectrum. Integrating this function over z , we find the overall spectral overlap function. From Fig.6 we see that in case of a 5 mm BBO crystal at collinear degenerate phase matching, only a relatively narrow wavelength range

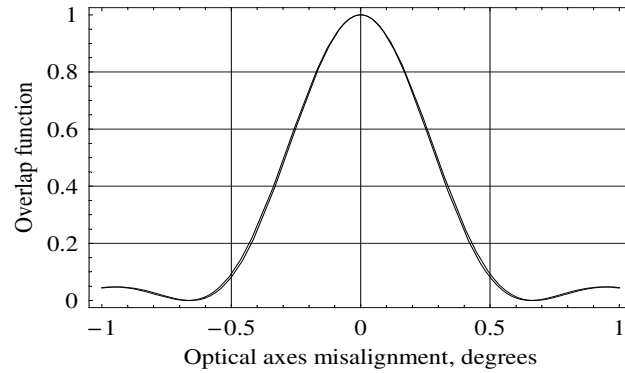


Figure 5: The overlap function vs. misalignment of optical axes of two crystals.

can be efficiently up-converted. As a result, the above estimate of 40 photons per second is considerably reduced. These and other difficulties have so far precluded a convincing experimental demonstration of biphoton detection via optical up-conversion, however we plan to continue our work in this direction.

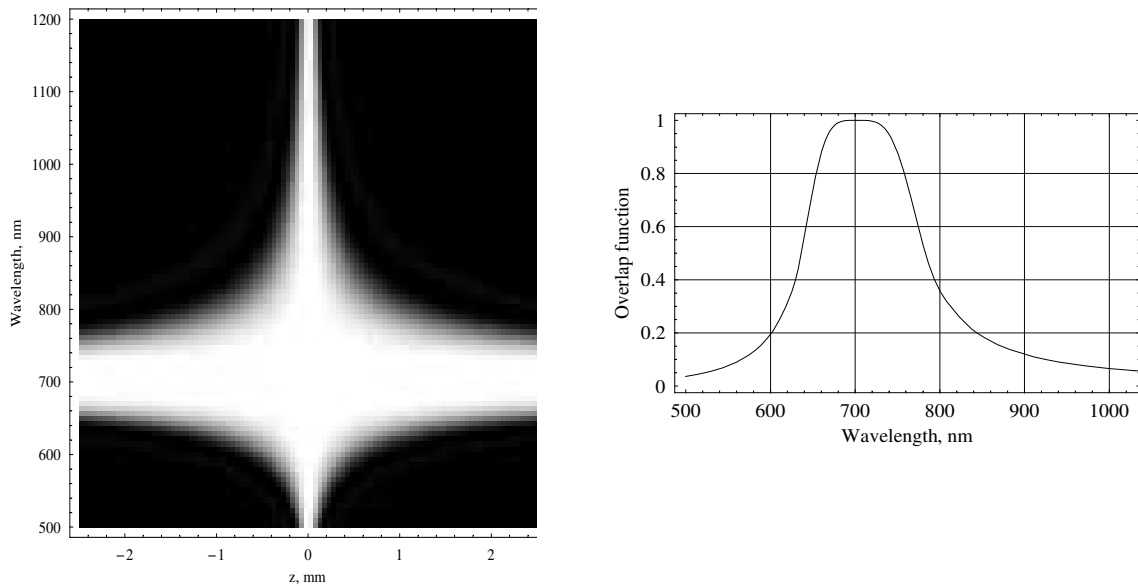


Figure 6: Left: the overlap function vs. the displacement z from the imaging plane and the wavelength. Right: the overlap function for a 5 mm crystal vs. the wavelength.

4 Photo-electric processes in a biphoton field

Another system interesting for the study of two-photon processes is a metal or semiconductor surface. If the red threshold of the external photo-electric effect in such a system corresponds to the total energy of the photon pair, one can expect a detectable photo-current corresponding to two-photon processes in the near absence of single-photon photo-current. The advantage of this system over the optical up-conversion is a much larger possible two-photon response cross-section; the disadvantage is that, in practice, such systems are very hard to characterize due to their complexity and a large number of simultaneously occurring physical processes.

The two-photon response of the photocathodes in photo-multiplier tubes (PMT) has been studied for use in the characterization of temporal properties of ultrafast laser pulses in which the peak intensity is extremely large [34,35]. Two-photon ionization may proceed by a direct two-photon channel via a virtual level, or by an indirect (cascade) process in which the electron may reside in an intermediate state, such as the conduction band or a deep trap, for some period of time. In many cases it may be beneficial to have an intermediate state in single-photon resonance with the light, because it increases the two-photon absorption rate. However, for the observation of two-photon light from SPDC, long-lived intermediate states may lead to a signal from uncorrelated photons, which is undesirable. The purpose of this work is to characterize a potential material for two-photon detection and to develop an understanding of the relevant physics for optimizing a fast two-photon detector. We are interested in observing the two-photon photo-electric effect from biphoton light, initiated by quantum-correlated photon pairs, rather than by absorption of statistically independent pairs of photons. For efficient discrimination between these two competing processes, we need to make sure the longest lifetime of the intermediate states is not much longer than the biphoton correlation time.

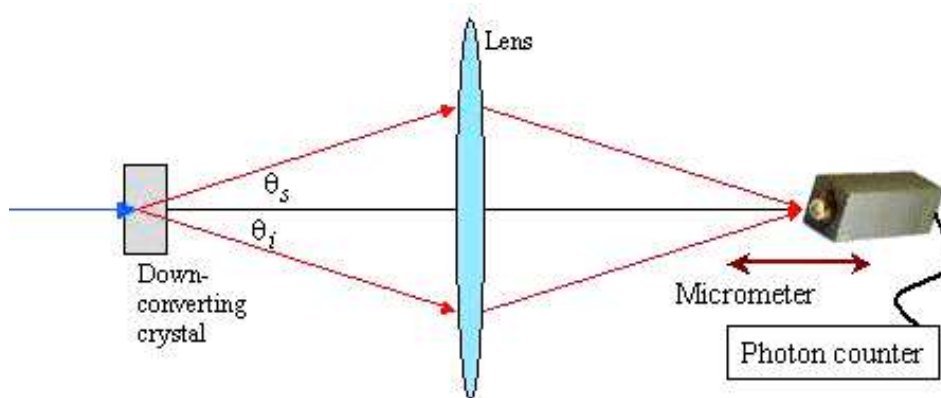


Figure 7: Illustration of the two-photon photocathode experiment with biphoton light.

In our experiment, we image the biphoton source onto a Cs_2Te photocathode with diffraction-limited resolution, as illustrated in Fig.7. We use a PerkinElmer MH922P channel photomultiplier detector in photon counting mode. This CPM has a Cs_2Te cathode

which has a bandgap of 3.3 eV and electron affinity of less than 0.5 eV [36]. The peak quantum efficiency, centered at 200 nm, is about 0.1. It falls off to approximately 10^{-3} at our pump wavelength (351.1 nm Argon Ion laser line), and to 10^{-8} at 702 nm, the degenerate signal and idler wavelength. Therefore one might expect to see a two-photon response from our SPDC biphoton source. If the short-wavelength part of the SPDC spectrum is suppressed, the single-photon response is expected to be very small. In our experiment, this part of the spectrum, along with the UV pump, was suppressed by narrow-band and by low-pass optical filters down to the dark noise of the PMT, which was at the level of a few counts per second. The PMT was moved in and out of the image plane. Although it always collected the same amount of light on its photocathode which, is 5 mm in diameter, all of the photon pairs are expected to focus to diffraction-limited spots only in the image plane. Therefore, the two-photon photo-electric signal should have a peak in the image plane. We have observed the expected behavior, see Fig.8. However, the origin of this peak turns out not to be due to the predicted two-photon effect, as discussed below.

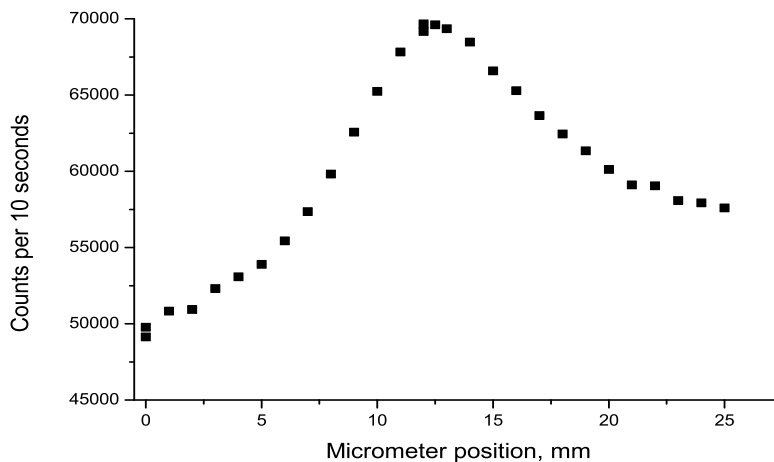


Figure 8: Two-photon PMT response to the biphoton SPDC light as a function of the PMT position in Fig.7.

Repeating the same experiment for attenuated CW laser light, we see a similar peak. Evidently, this peak arises from the fact that, in both the case of SPDC and the ordinary laser, the illuminated spot is the smallest, and therefore the intensity is the highest, in the image plane. Since the total light power is independent of the photocathode position, we obviously have some kind of a nonlinear (two-photon) process. This process, however, is very slow, which corresponds to a very large longitudinal extent of the two-photon detection volume. Physically, this most likely corresponds to a long lifetime of some intermediate state. As a result, a tight temporal (longitudinal) correlation of the biphoton field gives it no advantage over the attenuated classical light that has photons with Poissonian statistics.

Trying to determine the intermediate state lifetime, to characterize our prospective

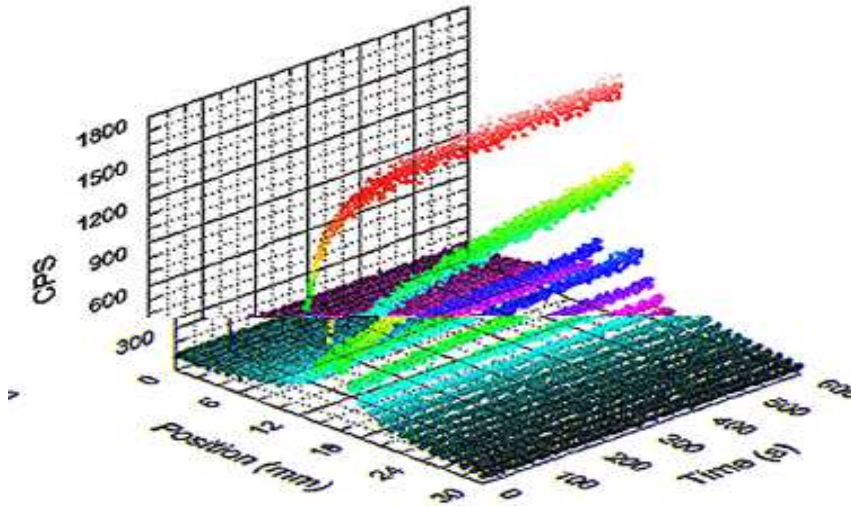


Figure 9: Dependence of the two-photon counting rate (in counts per second) on the photocathode position with respect to the lens and on time.

two-photon detector, we found that its two-photon sensitivity itself depends on time. This dependence is stronger for higher light intensities, that is, near the image plane. The situation can be described as the two-photon self-sensitization, which is illustrated in Fig.9 for an attenuated diode laser at around 650 nm. From Fig.9 we can see that the sensitization rate is higher for a higher intensity and that for the maximum light level we used (1.4 nW focused in a spot of 35 μm in diameter) the two-photon sensitivity can be increased by more than an order of magnitude over a period of time of about 100 seconds, at which point it saturates. We have also observed qualitatively similar power-dependent sensitization effect when keeping the illuminated area constant but changing the light power. However the preference was given to the other method because of experimental convenience.

The photocathode remains saturated for some time after the light is turned off. Its relaxation back to the initial unsaturated sensitivity, as a function of time, is shown in Fig.10. To obtain this dependence, we have sensitized the photocathode at the maximum light level, and then let it sit in the dark, while periodically probing its response with weak light pulses. This response has been normalized to the probe light photon flux to yield directly the quantum efficiency. We found that the resulting decay curve fits to a bi-exponential function with decay constants of around 100 and 5 seconds, which may indicate the presence of at least two intermediate states. A possible explanation is that the electrons undergo indirect single-photon transition into deep trapped states in the bandgap. The nature of these states is unclear to us at this point. These could be surface states as well as localized impurity states, or the states associated with structural defects. In support of the deep-state hypothesis, we should mention the experimental observations of the photoconductivity dynamics in GaAs [37]. In this experiment, filling the deep traps by the photo-activated electrons from a valence band results in a life-time increase of the

electrons in the conduction band. The activation and relaxation time scales in this process are close to what we observe for Cs_2Te .

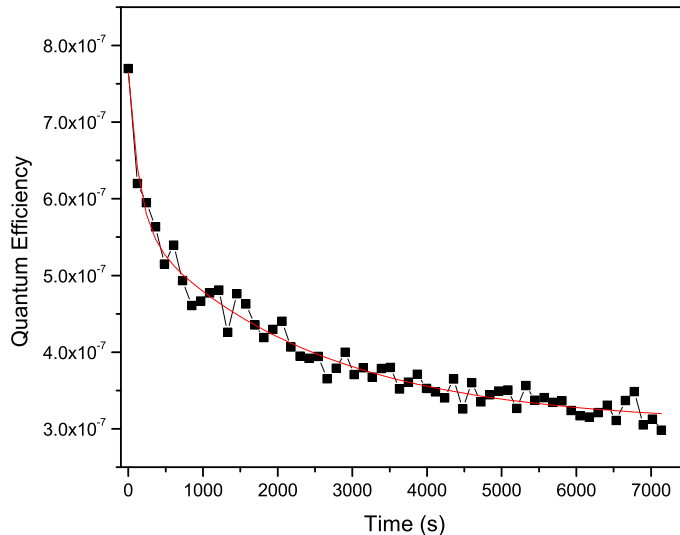


Figure 10: Relaxation curve for a self-sensitized Cs_2Te photo cathode.

5 Conclusions and perspectives

We have considered two types of two-photon processes that can be demonstrated with a faint biphoton field from SPDC and may in principle enable a fast two-photon detector: a process of coherent frequency up-conversion in an optically nonlinear media, and a two-photon photo-electric effect on a semiconductor photo-cathode. This is far from a complete list of processes that can be studied in this context. As the most obvious examples of the two-photon processes left beyond the scope of the present work, we would like to mention the internal photo-electric effect in broad-bandgap semiconductors; the earlier-mentioned ionization of alkali gases [24, 25]; and photo-chemical processes such as two-photon fluorescence and polymerization, e.g. [38].

Internal two-photon photo-electric processes should be similar to the external ones with the only difference that for the former the excited photo electrons remain in the conduction band and do not get emitted into vacuum. The internal processes can occur at much further distances from the surface than the external ones. This may simplify description of the internal processes by allowing one to neglect the effects of surface states and surface-bound impurities. We plan on studying this effect and expect that understanding of the mechanisms accompanying the external two-photon photo-electric effect will help.

Two-photon ionization of hydrogen-like gases is an example of a process that could be described analytically. Its simplicity is very attractive for research, however extremely

low detection cross section, resulting from a low concentration of atoms in a gas, presents a serious experimental challenge in the case of a faint biphoton field. In photo-chemical fluorescence processes, on the other hand, the two-photon cross-section of an individual molecule can be quite large (reaching $1,250 \times 10^{-50} \text{ cm}^4 \text{ s}$ per photon [38]), while the concentration of molecules is also much larger than in gases. The two-photon polymerization is a subject of a great interest, since this is the key to the quantum two-photon lithography. While the two-photon polymerization of specially designed photoresists with strong laser pulses has been successfully demonstrated by several groups, e.g. [38–40], the attempts to reproduce the same effect with biphoton field have not so far succeeded. While there are still several questions concerned with the photoresists properties (such as the reciprocity failure for long exposures, the role of thermal mechanisms, etc.) that need to be studied in order to achieve the success, the present study helps to answer one of the key questions by exploring the transverse correlation properties of the biphoton light. Specifically, for any particular imaging system, the transverse correlation function $F(0, \Delta\theta_s, \Delta\theta_i)$ that we have studied can be converted from the angular to linear variables $F(0, \Delta\rho_s, \Delta\rho_i)$ which has a direct relevance for calculating the two-photon exposure doses in quantum lithography.

Acknowledgments

This work was carried out at the Jet Propulsion Laboratory, California Institute of Technology, under a contract with the National Aeronautics and Space Administration. We would also like to acknowledge financial support from the Office of Naval Research, the National Security Agency, the National Reconnaissance Office, the Advanced Research and Development Activity, and the Defense Advanced Research Projects Agency. We appreciate fruitful discussions with S.P. Kulik and A.N. Penin.

References

- [1] D.N. Klyshko. Transverse photon bunching and two-photon processes in the field of parametrically scattered light. *Sov. Phys. JETP*, **56**:753–59, (1982).
- [2] J.A. Giordmaine and R.C. Miller. Tunable coherent parametric oscillation in LiNbO_3 at optical frequencies. *Phys. Rev. Lett.*, **14**:973–6, (1965).
- [3] A.V. Burlakov, M.V. Chekhova, D.N. Klyshko, S.P. Kulik, A.N. Penin, Y.H. Shih, and D.V. Strekalov. Interference effects in spontaneous two-photon parametric scattering from two macroscopic regions. *Phys. Rev. A*, **56**:3214–25, (1997).
- [4] A.V. Burlakov, M.V. Chekhova, O.A. Karabutova, and S.P. Kulik. Biphoton interference with a multimode pump. *Phys. Rev. A*, **63**:053801, (2001).
- [5] T.B. Pittman, D.V. Strekalov, A. Migdall, M.H. Rubin, A.V. Sergienko, and Y.H. Shih. Can two-photon interference be considered interference of two photons? *Phys. Rev. Lett.*, **77**:1917–20, (1996).

- [6] D.V. Strekalov, T.B. Pittman, and Y.H. Shih. What we can learn about single photons in a two-photon interference experiment. *Phys. Rev. A*, **57**(1):567–570, Jan (1998).
- [7] A. Einstein, B. Podolsky, and N. Rosen. Can quantum mechanical description of reality be considered complete? *Phys. Rev.*, **35**:777–780, (1935).
- [8] Pan JW, Bouwmeester D, Daniell M, Weinfurter H, and Zeilinger A. Experimental test of quantum nonlocality in three-photon greenberger-horne-zeilinger entanglement. *Nature*, **403**:515–519, (2000).
- [9] Bouwmeester D, Pan JW, Mattle K, Eibl M, Weinfurter H, and Zeilinger A. Experimental quantum teleportation. *Nature*, **390**:575–579, (1997).
- [10] Kim YH, Kulik SP, and Shih YH. Quantum teleportation of a polarization state with a complete bell state measurement. *Phys. Rev. Lett.*, **86**(7):1370–1373, Feb (2001).
- [11] A.K. Ekert. Quantum cryptography based on Bell’s theorem. *Phys. Rev. Lett*, **67**:661–663, (1991).
- [12] Yuen HP. Generation, detection, and application of high-intensity photon-number-eigenstate fields. *Physical Review Letters*, **56**:2176–79, (1986).
- [13] Yurke B, McCall SL, and Klauder JR. SU(2) and SU(1,1) interferometers. *Phys. Rev. A*, **33**:4033–54, (1986).
- [14] L.A. Lugiato, A. Gatti, and E. Brambilla. Quantum imaging. *J. Opt. B*, **4**:S1–S8, (2002).
- [15] R. Jozsa, D.S. Abrams, J. P. Dowling, and C. P. Williams. Quantum clock synchronization based on shared prior entanglement. *Phys. Rev. Lett.*, **85**:2010–13, (2000).
- [16] V. Giovannetti, S. Lloyd, and L. Maccone. Positioning and clock synchronization through entanglement. *Phys. Rev. A*, **65**:022309, (2002).
- [17] A.N. Boto, P. Kok, D.S. Abrams, S.L. Braunstein, C. P. Williams, and J.P. Dowling. Quantum interferometric optical lithography: exploiting entanglement to beat the diffraction limit. *Phys. Rev. Lett.*, **85**:2733–36, (2000).
- [18] P. Kok, A.N. Boto, D.S. Abrams, C. P. Williams, S. L. Braunstein, and J. P. Dowling. Quantum interferometric optical lithography: Towards arbitrary two-dimensional patterns. *Phys. Rev. A*, **63**:063407, (2001).
- [19] Bjork G, Sanchez-Soto LL, and Soderholm J. Entangled-state lithography: Tailoring any pattern with a single state. *Phys. Rev. Lett.*, **86**:4516–19, (2001).
- [20] M. D’Angelo, M.V. Chekhova, and Y.H. Shih. Two-photon diffraction and quantum lithography. *Phys. Rev. Lett.*, **87**:013602, (2001).

- [21] D.V. Strekalov and J.P. Dowling. Two-photon interferometry for high-resolution imaging. *J. of Mod. Opt.*, **49**:519–527, (2002).
- [22] G. Gilbert and M. Hamrick. Practical quantum cryptography: A comprehensive analysis (part one). *quant-ph/0009027*, (2000).
- [23] I. Abram, R.K. Raj, J.L. Oudar, and G. Dolique. Direct observation of the second-order coherence of parametrically generated light. *Phys. Rev. Lett.*, **57**:2516–2519, (1986).
- [24] N. Ph. Georgiades, E. S. Polzik, K. Edamatsu, and H. J. Kimble. Nonclassical excitation for atoms in a squeezed vacuum. *Phys. Rev. Lett.*, **19**, (1995).
- [25] N.P. Georgiades, E.S. Polzik, and H.J. Kimble. Quantum interference in two-photon excitation with squeezed and coherent fields. *Phys. Rev. A*, **59**:676–690, (1999).
- [26] J. Perina. *Coherence of light*. D. Reidel Publishing Comp., 2nd edition, (1985).
- [27] D.N. Klyshko. *Photons and Non-linear Optics*. Gordon and Breach Science, New York, 1988.
- [28] Y.H. Shih and C.O. Alley. New type of Einstein-Podolsky-Rosen experiment using pairs of light quanta produced by optical parametric down conversion. *Phys. Rev. Lett.*, **61** :2921–2924, (1988).
- [29] C.K. Hong, Z.Y. Ou, and L. Mandel. Measurement of subpicosecond time intervals between two photons by interference. *Phys. Rev. Lett.*, **59**:2044–2046, (1987).
- [30] M.H. Rubin. Transverse correlation in optical spontaneous parametric down conversion. *Phys. Rev. A*, **54**:5349, (1996).
- [31] A.F. Abouraddy, B.E.A. Saleh, A.V. Sergienko, and M.C. Teich. Role of entanglement in two-photon imaging. *Phys. Rev. Lett.*, **87**:123602, (2001).
- [32] M.B. Nasr, A.F. Abouraddy, M.C. Booth, B.E.A. Saleh, A.V. Sergienko, M.C. Teich, M. Kempe, and Ralf Wolleschensky. Biphoton focusing for two-photon excitation. *Phys. Rev. A*, **65**:023816, (2002).
- [33] Y.H. Shih, A.V. Sergienko, M.H. Rubin, T.E. Kiess, and C.O. Alley. Two-photon entanglement in type-II parametric down-conversion. *Phys. Rev. A*, **50**:23–28, (1994).
- [34] C.Rulliere, editor. *Femtosecond Laser Pulses, Principles and Experiments*. Springer-Verlag, (1998).
- [35] T. Hattori, Y. Kawashima, M. Daikoku, H. Inouye, and H. Nakatsuka. Femtosecond two-photon response dynamics of photomultiplier tubes. *Jpn. J. Appl. Phys.*, **39**:4793–98, (2000).

- [36] R. A. Powell, W. E. Spicer, G. B. Fisher, and P. Gregory. Photoemission studies of cesium telluride. *Phys. Rev. B*, **8**:15, (1973).
- [37] B. Santic, U.V. Desnica, N. Radic, D. Desnica, and M. Pavlovic. Photoconductivity transients and photosensitization phenomena in semiinsulating GaAs. *J. of Appl. Phys.*, **73**:5181–84, (1993).
- [38] B.H. Cumpston *et al.* Two-photon polymerization initiators for three-dimensional optical data storage and microfabrication. *Nature*, **398**:51–54, (1999).
- [39] G.Witzgall, R. Vrijen, E. Yablonovitch, V. Doan, and B.J. Schwartz. Single-shot two-photon exposure of commercial photoresist for production of three-dimensional structures. *Optics Letters*, **23**:1745–47, (1998).
- [40] S. Kawata, H.-B. Sun, T. Tanaka, and K. Takada. Finer features for functional microdevices. *Nature*, **412**:697–98, (2001).